

2008

Switching behavior of a Stoner–Wohlfarth particle subjected to spin-torque effect

Dorin Cimpoesu
University of New Orleans

Alexandru Stancu

Leonard Spinu
University of New Orleans

Huy Pham
University of New Orleans

Follow this and additional works at: https://scholarworks.uno.edu/phys_facpubs



Part of the [Physics Commons](#)

Recommended Citation

J. Appl. Phys. 103, 07B105 (2008)

This Article is brought to you for free and open access by the Department of Physics at ScholarWorks@UNO. It has been accepted for inclusion in Physics Faculty Publications by an authorized administrator of ScholarWorks@UNO. For more information, please contact scholarworks@uno.edu.

Switching behavior of a Stoner–Wohlfarth particle subjected to spin-torque effect

Huy Pham

Department of Physics, University of New Orleans, New Orleans, Louisiana 70148, USA
Advanced Materials Research Institute (AMRI), University of New Orleans, New Orleans, Louisiana 70148, USA

Dorin Cimpoesu^{a)}

AMRI, University of New Orleans, New Orleans, Louisiana 70148, USA

Alexandru Stancu

“Al. I. Cuza” University, Department of Physics, Iasi 700506, Romania

Leonard Spinu^{b)}

Department of Physics, University of New Orleans, New Orleans, Louisiana 70148, USA
AMRI, University of New Orleans, New Orleans, Louisiana 70148, USA

(Presented on 8 November 2007; received 13 September 2007; accepted 13 October 2007; published online 1 February 2008)

Recently, the current-induced spin-transfer torque has been proposed as a convenient writing process in high density magnetic random access memory. A spin-polarized current can switch the magnetization of a ferromagnetic layer more efficiently than a current induced magnetic field. Our paper discusses the switching properties of a Stoner–Wohlfarth magnetic particle for the case when spin torques and external field pulses are simultaneously present. The theoretical investigation of precessional motion is described by using Landau–Lifschitz–Gilbert equation with a spin-transfer torque term included. The main goal is to determine the parameters of field pulse for that the fast and stable switching can be achieved. © 2008 American Institute of Physics.

[DOI: [10.1063/1.2830720](https://doi.org/10.1063/1.2830720)]

I. INTRODUCTION

The concept of the “spin-transfer torque” proposed by Slonczewski¹ and Berger² offers a new way of controlling the magnetization reversal in ferromagnetic multilayer systems, which replaces the conventional method utilizing magnetic field. The transfer of the spin angular momentum between two magnetic layers by the current flowing perpendicular to plane can reverse the magnetization of one of the magnetic layers. The novel technology utilizing the spin-transfer torque is expected to reduce the switching time of magnetization as well as to increase the recording density of the magnetoresistive random access memories^{3–6} (MRAMs) and other data storage devices. Devolder *et al.*^{7,8} proposed to bias the free layer with a hard axis field, in order to obtain a reproducible subnanosecond duration when the free-layer easy axis is parallel to the spin polarization of the current. However, the precise nature of magnetization dynamics when spin-polarized current and external pulsed field are simultaneously present has not been well studied.

In this paper the switching properties of a Stoner–Wohlfarth particle, subject to a continuous or short magnetic field pulse, and to a short current pulse, obtained by numerical investigations, are presented. The switching is discussed

as a function of the applied field strength and direction, and as a function of the length of the current pulse. Finally, the case of asynchronously pulses is discussed.

II. MODEL

In typical spin-transfer investigation, the electron current is sent along the z direction across a metallic multilayer element with layers parallel to the (x, y) plane. The element consists of a so-called “fixed” magnetic layer with magnetization pinned along the x axis, a nonmagnetic spacer, and a “free” magnetic layer exposed to the torque due to x -directed spin polarization that the electrons acquire from fixed layer. The dynamic behavior of the magnetization of the free layer is governed by the modified Landau–Lifshitz–Gilbert equation with spin-transfer term included.^{1,2} This equation can be written in dimensionless form as

$$\frac{d\mathbf{m}}{dt} = \alpha \mathbf{m} \times \frac{d\mathbf{m}}{dt} - \mathbf{m} \times (\mathbf{h}_{\text{eff}} - \beta \mathbf{m} \times \mathbf{e}_p), \quad (1)$$

where the free-layer magnetization \mathbf{m} and the effective field \mathbf{h}_{eff} are normalized by the saturation magnetization M_s , time is measured in units of $(\gamma M_s)^{-1}$, $\gamma = 2.211 \times 10^5$ (rad/s)/(A/m) is the gyromagnetic ratio, α is the phenomenological damping constant, the unit vector \mathbf{e}_p gives the direction of the spin polarization (along x direction in our case), and β is proportional to the current density J_e as follows: $\beta = \hbar J_e / 2 |e| M_s^2 d$, where e is the electron charge, d is the thickness of the free layer, and \hbar is the Planck constant. The

^{a)}Permanent address: “Al. I. Cuza” University, Department of Physics, Iasi 700506, Romania.

^{b)}Author to whom correspondence should be addressed. Electronic mail: LSpinu@uno.edu.

parameter β is positive when the electrons flow from the free into the fixed layer. The effective field consists of applied field and demagnetizing field, no further anisotropy being considered.

As ferromagnetic material, Co with $4\pi M_S = 12$ kG and $\alpha = 0.01$ was chosen. The free magnetic layer is assumed to be ellipsoid shaped, making the demagnetizing field uniform across the entire layer. The ellipsoid's principal axes are taken along x , y , and z : long-axis length of 100 nm (along Ox axis), short-axis length of 75 nm (along Oy axis), and thickness $d = 2$ nm, leading to demagnetizing factors $N_x = 0.014$, $N_y = 0.022$, and $N_z = 0.964$.

All calculations presented in the following are performed for a maximum value of the current pulse of 0.5 mA (i.e., $|\beta| = 1.22 \times 10^{-2}$). The results are obtained by numerical integration of Eq. (1) using a standard, self-optimizing, embedded Runge–Kutta algorithm.

III. RESULTS

A. Precession of the magnetization in a dc applied field and a pulsed current

In this section, the switching of the magnetization under application of a dc magnetic field and of a pulse of current is discussed. For the current pulse rise and fall sinusoidal time dependence is assumed, and the pulse is characterized by the triplets of numbers “rise time/pulse length/fall time,” with all values given in units of nanoseconds, the pulse length being defined as interval between the time when the pulse reaches $1/\sqrt{2}$ of its amplitude, and the time when the pulse drops to the same value.

In order to characterize the precessional switching of magnetization subjected to a dc applied magnetic field with different strengths and orientations, taking into account also the effect of spin-transfer torque, we have used the switching diagram proposed by Bauer *et al.*,⁹ in which the final value of the projection m_x of the magnetization vector is displayed as a function of the strength and direction of the applied field. In Fig. 1 different scenarios of the magnetization switching in the nonpresence/presence of the spin-transfer torque, initiated by a dc magnetic field, are shown. Prior to the applied field, the magnetization lies along negative x direction and the color in grayscale from black to white on the diagram indicates the final state of m_x : black areas represent $m_x = -1$ (nonswitching), white areas represent $m_x = 1$, and the intermediate values of m_x are represented with shades of gray. Figure 1(a) represents the switching diagram in the case when no spin-transfer torque is included. One can observe that switching is induced only when the applied field has a component along the positive x direction, and the separation boundary between black and white, corresponding to switched and nonswitched regions, is very well defined, forming an astroidlike shape. The dramatic changes are easily observed in the switching diagrams in the case taking into account the spin-transfer torque term with different current pulse lengths [see Figs. 1(b)–1(d)].

Increasing the current pulse length, the white color region enlarges gradually to the left, gnawing the astroidlike region, and the switching can be induced also by a field with

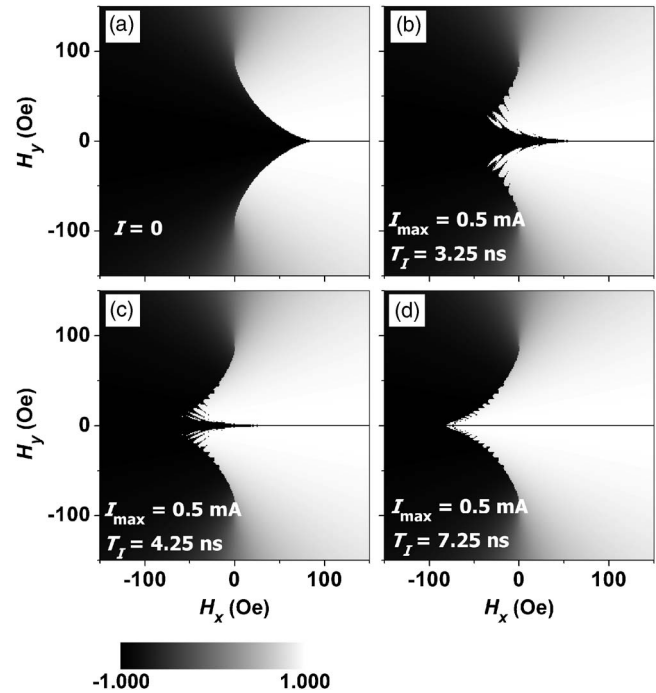


FIG. 1. Switching diagram as a function of the applied dc field, for different values of the current pulse length $0.25/T_f/0.25$: (a) no current applied, (b) $T_f = 3.25$ ns, (c) $T_f = 4.25$ ns, and (d) $T_f = 7.25$ ns. The direction of the spin polarization (pinned layer) is along the negative x direction and the initial direction of magnetization is also along the negative x direction ($m_x = -1$). Black areas represent $m_x = -1$ (nonswitching), white areas represent $m_x = 1$, and the intermediate values of m_x are represented with shades of gray. The maximum value of the current pulse is 0.5 mA.

a negative component along the x direction. One observes that for the longest current pulse [see Fig. 1(d)] almost entire interior region of the astroid switches.

From Fig. 1 we can see that even if the supplementary current-induced torque is equivalent with a variable field, the global effect on the switching diagram is not a translation of the diagram, but a deformation on the x direction, with maximum deformation at $H_x = 0$.

B. Precession of the magnetization in a pulsed applied field and a pulsed current

In this section we describe the switching of the magnetization in a pulsed field and a pulsed current applied synchronously and asynchronously, respectively. Instead of the final state of m_x , now we map the switching time, defined as the time required for the magnetization to approach the equilibrium position along the positive x axis, until the torque acting on the magnetization becomes negligible (there is no significant ringing), after the cutoff of both pulses. In Figs. 2 and 3 the black areas represent no switching, and the gray level is scaled from dark gray for 6 ns to white for 12.5 ns. We now apply a $0.25/0.25/0.25$ pulse of field, and construct the switching diagrams of magnetization for different cases of the pulse length of the current pulse. The result is displayed in Fig. 2. The final state is determined by the position of the magnetization when the field pulse and the spin-current pulse are terminated. The switching time is found in the range of few nanoseconds. Figures 2(b)–2(d) show that as the time length of current pulse increases, the regions of

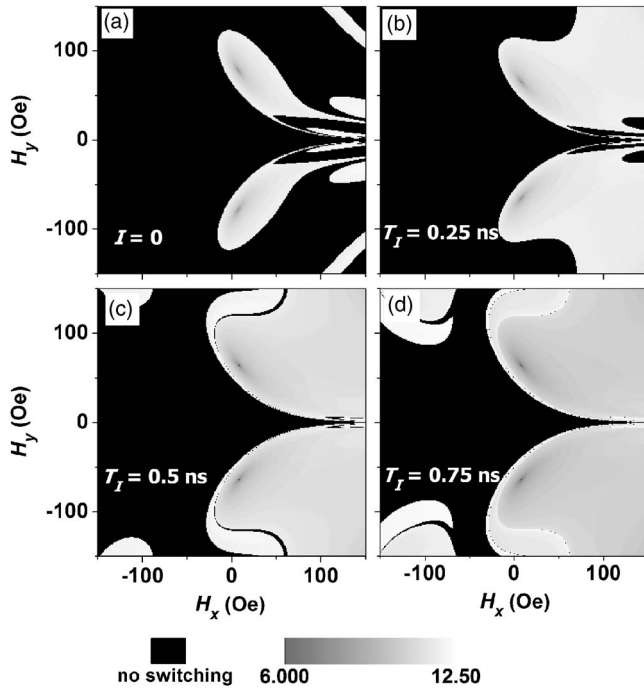


FIG. 2. Time switching as a function of the maximum value of a pulse field with the length 0.25/0.25/0.25, for different values of the current pulse length $0.25/T_I/0.25$: (a) no current applied, (b) $T_I=0.25$ ns, (c) $T_I=0.5$ ns, and (d) $T_I=0.75$ ns. Black areas represent no switching, and the gray level is scaled from dark gray for 6 ns to white for 12.5 ns.

stable switching into the positive x direction are enlarged compared to the case of no spin-transfer current applied, as shown in Fig. 2(a). It is clear that the longer the pulse duration of the spin-transfer current, the stronger effects of spin torque on switching diagram are observed. We come up to a conclusion that the spin torque plays a very important role in driving switching of the magnetization. Improved switching of a MRAM cell, therefore, could be achieved by simultaneously addressing the short pulse of field and pulse of current.

If in Fig. 2 the current pulse is starting at the same time with the pulse of field (synchronously), let us now investigate the influence of the starting time of the current pulse, which is denoted as t_1 , on the magnetization reversal. In Fig. 3(a) the current pulse starts when the field pulse reaches its maximum value of the sinusoidal form. The white region (the switching region) is enlarged compared with the case of synchronous pulses [Fig. 2(b)]. If the pulse of current starts when the pulse of field is finished [see Fig. 3(b)] the switching region decreases again. Moreover, the pulse current delay is a critical parameter in the switching behavior, as it can be observed from the bottom panels of Fig. 3. Thus, points A and B with the same field pulse but different t_1 delays have different switching outcomes, with point B remaining in the initial state (no-switching) and point A switching.

IV. CONCLUSIONS

The dynamic behavior of magnetization under the competitive torques of a spin-polarized current and an external magnetic field has been derived. Our calculations are useful

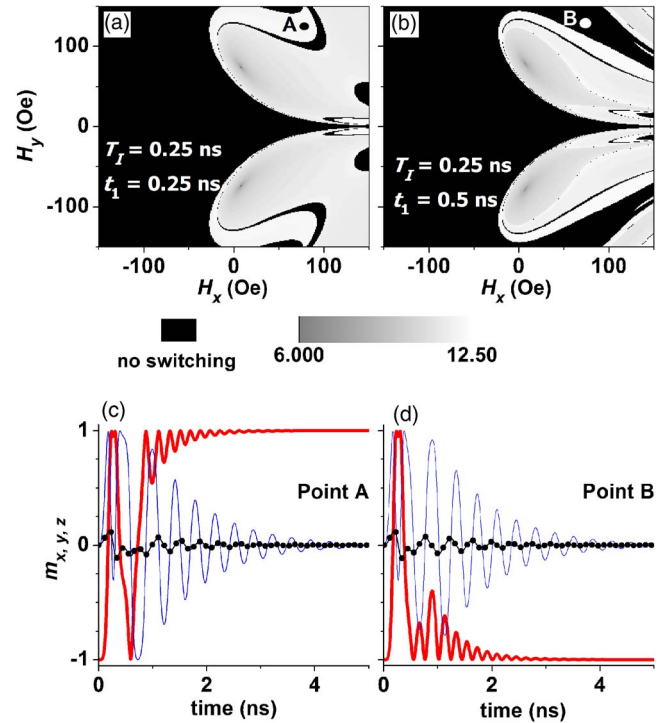


FIG. 3. (Color online) Time switching as a function of the maximum value of a pulse field with the length 0.25/0.25/0.25, and for a current pulse with the length 0.25/0.25/0.25 starting at the moment t_1 : (a) $t_1=0.25$ ns and (b) $t_1=0.5$ ns. Black areas represent no switching, and the gray level is scaled from dark gray for 6 ns to white for 12.5 ns. [(c) and (d)] Time evolution of m_x (bold line), m_y (thin line), and m_z (symbols) at the positions A and B indicated in the top diagrams.

to develop an understanding of the current-induced magnetic switching. It is seen from diagram presentations that the switching properties are strongly enhanced by the presence of the spin-transfer torque. Reversal processes can become complex, but switching regions are enlarged. Also, it was shown that the switching behavior is strongly dependent on timing of the field and current pulses, i.e., synchronous or asynchronous.

ACKNOWLEDGMENTS

Work at AMRI was supported by DARPA under Grant No. HR0011-07-1-0031. Calculations were performed on computational facilities provided by Louisiana Optical Network Initiative (<http://www.loni.org>) which is supported by the Louisiana Board of Regents. This work was partially supported by Romanian CNCSIS under the Grant A(RELSWITCH).

¹J. C. Slonczewski, J. Magn. Magn. Mater. **159**, L1 (1996).

²L. Berger, Phys. Rev. B **54**, 9353 (1996).

³J. C. Slonczewski, U.S. Patent No. 5,695,864 (9 December 1997).

⁴M. Hosomi *et al.*, Tech. Dig. - Int. Electron Devices Meet. **2005**, 459.

⁵Y. Huai and P. P. Nguyen, U.S. Patent No. 6,920,063 B2 (19 July 2005).

⁶F. B. Mancoff, B. N. Engel, and N. D. Rizzo, U.S. Patent No. 7,149,106 B2 (12 December 2006).

⁷T. Devolder, C. Chappert, J. A. Katine, M. J. Carey, and K. Ito, Phys. Rev. B **75**, 064402 (2007).

⁸T. Devolder, C. Chappert, and K. Ito, Phys. Rev. B **75**, 224430 (2007).

⁹M. Bauer, J. Fassbender, and B. Hillebrands, Phys. Rev. B **61**, 3410 (2000).